FACTA UNIVERSITATIS
Series: **Mechanical Engineering**
https://doi.org/10.22190/FUME241116016S

Original scientific paper

OPTIMIZING NON-INVASIVE REMOTE SENSING FOR GEOTHERMAL EXPLORATION WITH T-SPHERICAL DUAL HESITANT FUZZY DECISION MODEL

Michael Sandra[1], Samayan Narayanamoorthy[1], Krishnan Suvitha[2], Dragan Pamucar[3,4,5], Daekook Kang[6]

[1]Department of Mathematics, Bharathiar University, Coimbatore, India
[2]Centre for Nonlinear Systems, Chennai Institute of Technology, Chennai, Tamilnadu, India
[3]Department of Operations Research and Statistics, Faculty of Organizational Sciences, University of Belgrade, Belgrade, Serbia
[4]Department of Industrial Engineering & Management, Yuan Ze University, Taoyuan City, Taiwan
[5]Department of Applied Mathematical Science, College of Science and Technology, Korea University, Sejong, Republic of Korea
[6]Department of Industrial and Management Engineering, Institute of Digital Anti-aging Health care, Inje University, Gyeongsangnam-do, Republic of Korea

Abstract. *Traditional geothermal detection methods, such as extensive ground-based surveys and drillings, are often costly, time-consuming, and environmentally intrusive. To address these challenges, this study presents a novel hybrid fuzzy multi-criteria decision-making model to evaluate and prioritize non-invasive, cost-effective remote sensing (RS) techniques. This model uses T-spherical dual-hesitant fuzzy set to manage the inherent ambiguities in the evaluation of multiple criteria. The logarithmic percentage change-driven objective weighting technique assigns the relative importance of criteria, and the multiple triangle scenarios-II methodology helps in comprehensive evaluation and ranking. By incorporating expert judgment and addressing inherent uncertainties, this model provides a systematic framework for optimizing RS technique selection. Findings indicate that thermal infrared imaging, with a significance score of 0.7187, holds transformative potential for geothermal energy development. Sensitivity and comparative analyses further confirm the robustness of this approach. This research offers a valuable resource for energy developers and policymakers aiming to leverage RS technologies for efficient geothermal resource management and development.*

Key words: *MCDM, T-spherical dual-hesitant fuzzy set, Multiple triangles scenarios-II, Objective weighting, Geothermal detection*

Received: November 16, 2024 / Accepted April 08, 2025
Corresponding authors: Samayan Narayanamoorthy, Dragan Pamucar, Daekook Kang
Department of Mathematics, Bharathiar University, Coimbatore, India
E-mail: snmphd@buc.edu.in, dpamucar@gmail.com, dkkang@inje.ac.kr

1. INTRODUCTION

The global population is projected to reach 9.7 billion by 2050 [1], presenting significant challenges in meeting the escalating energy demands driven by increased urbanization, industrialization, and technological advancements. The depletion of conventional energy sources such as coal, petroleum, and natural gas not only threatens to exacerbate global warming but also poses severe environmental risks [2]. According to Chhandama et al., [3], carbon dioxide (CO_2) emissions are expected to reach 40 million kilograms by 2030, potentially contributing to a rise in global temperatures exceeding 2^0C. This abrupt upsurge in temperature could lead to the extinction of up to 1 million species and place hundreds of millions of humans at risk. Furthermore, it is predicted that around 50,000 TW of electrical energy will be required by 2050 [4], underscoring the urgent need for sustainable energy solutions. Immediate and sustainable interventions are essential to replenish these supplies and mitigate the associated environmental impacts to avert the impending energy crisis.

Renewable energy (RE) offers a sustainable alternative to finite resources, meeting growing energy demands while reducing environmental impact. Among RE sources, the transition to geothermal energy (GE) is particularly crucial due to its stability and reliability. Unlike solar and wind, GE provides a consistent energy supply, unaffected by weather variability, making it a crucial solution for seamless grid integration and long-term decarbonization. Despite being underutilized, GE's potential to deliver dependable, low-emission power highlights its importance in advancing the energy transition and ensuring sustainable energy security.

GE originates from the vast reservoir of thermal energy generated by the radioactive decay of minerals and the primordial heat from the Earth's formation. As a non-variable and renewable resource, GE can be used for baseload power generation, reducing overdependence on fossil fuels and hydropower plants [5]. Compared to other energy sources, the Earth has an essentially infinite supply of this energy stored within its core. This thermal energy is particularly abundant around the Pacific Ocean, including the Northern Hemisphere, where active volcanic regions contribute to significant geothermal resources. Effective exploitation of these resources requires thorough exploration.

Research into GE exploration has heavily relied on standard methods such as geophysical [6], geospatial [7], and electromagnetic [8] techniques. However, unanticipated geological intricacies and reservoir characteristics that were not accounted for during the prediction process could present operational obstacles or safety hazards during extraction, exacerbating the effects of erroneous predictions. Therefore, ensuring precise and reliable projections of geothermal reserves is critical for increasing energy production, efficiency, enhancing safety, and ensuring the long-term sustainability of this significant RE resource. Remote sensing (RS) has the potential to accurately identify locations showing geothermal anomalies [9]. Prospective geothermal sites can be found in remote or challenging terrains due to RS, which provides an inexpensive and non-invasive way to explore large, often inaccessible areas. There are distinct types of RS techniques, such as ASTER and TIR, applicable in various circumstances. By utilizing satellite or aerial sensors, RS can detect subtle temperature anomalies and surface manifestations associated with geothermal activity. Evaluating and selecting RS techniques involves multiple, often conflicting criteria, necessitating a multicriteria model for efficient use of GE. Multi-

Criteria Decision Making (MCDM) can help identify the most beneficial alternative by balancing these conflicting factors [10].

The limited availability of non-renewable resources presents a significant challenge in balancing future energy demand and production. This underscores the urgent need for more sustainable energy solutions. However, there is a notable gap in the existing literature regarding the optimal selection of RS techniques for geothermal reservoir exploration. Current methods for evaluating RS techniques often fail to fully capture the complexities of expert preferences, especially across large and diverse geographical areas. Additionally, MCDM models have limitations, including an inability to effectively convey expert assessments in natural language, and they tend to be time-consuming and inefficient. As a result, these models struggle to provide a decision order that reflects the real-world, in-depth process of human decision making (DM), hindering their effectiveness in selecting the most appropriate RS techniques for geothermal exploration.

The motivation for this study is to identify the optimal RS technique for geothermal reservoir exploration. To achieve this, a novel hybrid MCDM paradigm is introduced, applying a fuzzy approach to assess various RS techniques. However, choosing the ideal solution in MCDM is challenging due to inherent uncertainties, such as incomplete or ambiguous information, dynamic external factors, and the subjective judgments of decision-makers. By addressing these challenges, this study aims to improve decision-making processes, facilitating the efficient and accurate exploration of geothermal resources. This is crucial for advancing GE as a practical and reliable renewable energy source.

The novelty of this study lies in the development of a comprehensive decision-making framework that integrates the t-spherical dual hesitant fuzzy (T-SDHF) set to handle high uncertainty and hesitation, employs the logarithmic percentage change-driven objective weighting (LOPCOW) method for precise criterion weighting, and utilizes the multiple triangles scenarios-II (MUTRISS-II) technique for accurate alternative ranking. This is the first study to combine LOPCOW and MUTRISS-II for evaluating and selecting remote sensing techniques in geothermal reservoir exploration, offering a balanced and reliable assessment. The proposed approach is rigorously validated through robustness, sensitivity, and comparison analyses, ensuring its effectiveness in addressing complex decision-making challenges under imprecision and ambiguity.

2. Literature Review

In the multifaceted and constantly changing world of today, decision-makers face a slew of issues that necessitate an organized and well-informed process [11]. A systematic framework for handling decision issues combining numerous objectives, various criteria, and dynamic preferences is provided by MCDM techniques [12]. Traditional methods such as DEMATEL [13], VIKOR [14], TOPSIS [15], PROMETHEE [16], and ELECTRE [17] laid the groundwork by structuring decision problems, organizing options, and establishing preference relationships. However, as decision-making scenarios grew more intricate, newer techniques like WASPAS [18], COMET [19] and FRADAR [20] emerged. These advanced approaches better handle competing goals and incorporate subjective assessments from multiple decision-makers, providing a balanced and flexible framework that enhances decision quality and inclusiveness.

Some of the subjective weighting techniques include AHP [21], SWARA [22] while objective methods include entropy [23] and MEREC [24]. Besides these MCDM models, Ecer and Pamucar [25] introduced a novel objective weighting technique named LOPCOW. Its benefits include removing gaps in data because of the size, producing more realistic weightings, and taking into account positive as well as negative data when weighting. Tadic et al., [26] used modified fuzzy TOPSIS and fuzzy COPRAS methods for evaluation and ranking of electric vehicles. Nila et al., [27] employed triangular fuzzy LOPCOW-FUCOM technique for the evaluation and selection of third-party logistics service. Ulutas et al., [28] used grey numbers based LOPCOW framework for the evaluation of third-party logistic providers for automobile production firms. Biswas and Joshi [29] compared the post-listing performance of IPOs in the Indian Stock Market (ISM) using LOPCOW, highlighting that market performance is not solely driven by fundamental efficiency and equity ownership has little impact. The study suggested that other factors contribute to IPO performance beyond these traditional metrics.

Every MCDM technique that has been devised so far has encountered some restrictions such as the subjective nature of DM, reliance on data quality, and the challenge of model complexity [30]. To address these challenges, Zakeri et al., [31] presented a novel MCDM approach, MUTRISS-II that could compute the areas filled by options in n-dimensional space. The material selection challenges were addressed using this MUTRISS approach.

Making decisions frequently requires navigating subjectivity and ambiguity. Fuzzy-based MCDM techniques have been introduced to address unpredictability and inaccuracy in DM systems [32]. Multiple fuzzy sets (FS) have been proposed so far in the literature, including intuitionistic FS, interval-valued FS, neutrosophic FS, picture FS [33], bipolar FS, and linear-diophantine FS. However, among all of these FS, an innovative FS, spherical FS, introduce by Kutlu and Kahraman, has piqued the interest of academics due to the benefits it offers [34]. Bonab et al., [35] utilized spherical FS and choquet integral to evaluate autonomous cars for the logistics sector.

Nguyen et al., [36] assessed the wire and cable industry's governance, social, and environmental performance using the WASPAS and spherical fuzzy DEA-AHP approaches. Gamal et al. [37] developed an ecologically sound computational technique for evaluating the optimal energy storage systems by integrating AHP-MACONT in a spherical fuzzy environment. Spherical linear diophantine FS and its accompanying aggregated geometric and arithmetic operators were developed by Riaz et al. [38] in a study, and they are employed in many real-world applications, such as network systems, voting, digital image processing and so on. Further Kakati et al. [39] introduced rectified complex T-SF set employing the Dombi-Choquet integral operator to diagnose diabetic retinopathy through fundus images. Later, Alamoodi et al., [40] integrated 2-tuple linguistic T-SF set and entropy-FDOSM for the effective appraisal of electric bus.

Conventional models typically require experts to provide single values for membership parameters, which can be restrictive and less expressive, particularly in situations with competing criteria or uncertain evaluations. To address these issues, the T-SDHF set combines the t-spherical fuzzy (T-SF) and dual hesitant fuzzy (DHF) sets, incorporating positive, negative, and neutral membership functions. This integration allows T-SDHF sets to capture both degrees of membership and non-membership simultaneously, giving experts a more flexible and realistic way to convey hesitation and preferences. By doing so, the T-SDHF set improves the robustness of DM processes, providing a structured framework that can more

accurately reflect expert input and enhance the reliability of decision outcomes, even in intricate and high-dimensional DM scenarios.

MCDM techniques have proven effective in diverse fields such as business, engineering, healthcare, and energy, addressing complex decision-making challenges [41]. Their adaptability and versatility make them suitable for various decision-making scenarios. Mostafaeipour et al., [42] used the fuzzy-DELPHI-AHP methodology to investigate the difficulties in GE extraction in India. Using the SWARA-ARAS technique, Puppala et al., [43] investigated the location selection for geothermal projects in Afghanistan in 2022. Ghose et al., [44] then used triangular fuzzy TOPSIS technique to evaluate varied RE in India. Gudala et al., [45] used horizontal wells to analyse the Puga geothermal reservoir. A triplet of horizontal wells was evaluated and improved for CO_2 plume GE harvesting by Nematollahi et al., [46]. In their study, Ngethe et al., [47] examined the selection of GE resources for direct use in Kenya. In the northeastern region of Anatolia, Zorlu and Dede [48] assessed the possible geoheritage in glacial and periglacial deposits.

3. PRELIMINARIES

3.1. Dual Hesitant Fuzzy Set

A dual hesitant fuzzy (DHF) set defined on the Universal Set $\mho$ is represented by,

$$\rho = \left\{ \left\langle x, h(x), g(x) \right\rangle \mid x \in \mho \right\} \tag{1}$$

where, $h(x)$ and $g(x)$ are two sets of some values in [0,1] denoting the possible grades of membership and non-membership of the member $x \in \mho$ to the set ρ respectively, satisfying the condition

$$0 \le \zeta, \eta \le 1, 0 \le \zeta^{+} + \eta^{+} \le 1 \tag{2}$$

where $\zeta \in h(x)$, $\eta \in g(x)$, $\zeta^{+} \in h^{+}(x) = \mathrm{U}_{\zeta \in h(x)} \max \{\zeta\}$, $\eta^{+} \in g^{+}(x) = \mathrm{U}_{\eta \in g(x)} \max \{\eta\}$ for all $x \in \mho$. For ease, the pair $(h(x), g(x))$ is termed as DHF element denoted by $\Xi = (h,g)$, satisfying the condition, $\zeta \in h$, $\eta \in g$, $\zeta^{+} \in h^{+} = \mathrm{U}_{\zeta \in h} \max \{\zeta\}$, $\eta^{+} \in g^{+} = \mathrm{U}_{\eta \in g} \max \{\eta\}$, $0 \le \zeta, \eta \le 1$, $0 \le \zeta^{+} + \eta^{+} \le 1$.

3.2. T-Spherical Fuzzy Set

A t-spherical fuzzy (T-SF) set on $\mho$ is stated as,

$$T = \left\langle x, \left\{ \alpha_T(x), \beta_T(x), \gamma_T(x) \right\} \middle| \, x \in \mho \right\rangle \tag{3}$$

where, $\alpha_T(x) : \mho \to [0,1]$, $\beta_T(x) : \mho \to [0,1]$ and $\gamma_T(x) : \mho \to [0,1]$ signifies the positive grade of membership (PgM), abstain grade of membership (AgM) and negative grade of membership (NgM) to T respectively, fulfilling the condition,

$$0 \le \left(\alpha_T(x)\right)^n + \left(\beta_T(x)\right)^n + \left(\gamma_T(x)\right)^n \le 1 \tag{4}$$

for some Z_+ n with the triplet (α, β, γ) known as T-SF elements.

3.3. T-Spherical Dual Hesitant Fuzzy Set

A t-spherical dual hesitant fuzzy (T-SDHF) set on $\mho$ is defined by,

$$\varpi = \left\langle x, \left\{ \phi_{\varpi}(x), \mu_{\varpi}(x), \psi_{\varpi}(x) \right\} \middle| x \in \mho \right\rangle \tag{5}$$

where $\phi_{\varpi}(x)$, $\mu_{\varpi}(x)$, $\psi_{\varpi}(x)$ are three sets of some possible different values between [0,1] signifying PgM, AgM and NgM of the member $x \in \mho$ to the set ϖ respectively, with the condition,

$$0 \le \max\left(\phi_{\varpi}(x)\right)^n + \min\left(\mu_{\varpi}(x)\right)^n + \min\left(\psi_{\varpi}(x)\right)^n \le 1 \tag{6}$$

here $\phi_{\varpi}(x) = \max\{\Xi_{\phi}\}$, $\mu_{\varpi}(x) = \max\{\Xi_{\mu}\}$ and $\psi_{\varpi}(x) = \max\{\Xi_{\psi}\}$, in which Ξ_{ϕ}, Ξ_{μ} and Ξ_{ψ} are DHF elements for some Z_+ n. For convenience, the triplet $\phi_{\varpi}(x)$, $\mu_{\varpi}(x)$, $\psi_{\varpi}(x)$ is termed as t-spherical dual hesitant number (T-SDHFN) denoted by $\rho = (\phi, \mu, \psi)$. The refusal grade of membership is defined as,

$$\pi = \left[1 - \left\{ \left\{ \max\left(\phi_{\varpi}(x)\right) \right\}^n + \left\{ \min\left(\mu_{\varpi}(x)\right) \right\}^n + \left\{ \min\left(\psi_{\varpi}(x)\right) \right\}^n \right\} \right]^{\frac{1}{n}} \tag{7}$$

3.4. Score and Accuracy Function

The score function $S(\rho)$ and accuracy function $P(\rho)$ of T-SDHFN ρ are defined by,

$$S(\rho) = \frac{\left(1 + \left(\frac{1}{N(h_{\phi})}\sum_{i=1}^{N(\phi)} \zeta_{\phi} - \frac{1}{N(g_{\phi})}\sum_{i=1}^{N(\phi)} \eta_{\phi}\right)^n - \left(\frac{1}{N(h_{\psi})}\sum_{i=1}^{N(\psi)} \zeta_{\psi} - \frac{1}{N(g_{\psi})}\sum_{i=1}^{N(\psi)} \eta_{\psi}\right)^n\right)}{2} \tag{8}$$

$$P(\rho) = \frac{\left(1 + \left(\frac{1}{N(h_{\phi})}\sum_{i=1}^{N(\phi)} \zeta_{\phi} - \frac{1}{N(g_{\phi})}\sum_{i=1}^{N(\phi)} \eta_{\phi}\right)^n + \left(\frac{1}{N(h_{\psi})}\sum_{i=1}^{N(\psi)} \zeta_{\psi} - \frac{1}{N(g_{\psi})}\sum_{i=1}^{N(\psi)} \eta_{\psi}\right)^n\right)}{2} \tag{9}$$

where $N(h_{\phi})$, $N(g_{\phi})$, $N(h_{\psi})$, and $N(g_{\psi})$ represent the number of elements contained respectively in ϕ and ψ for some Z_+ n. The value of the $S(\rho) \in [0,1]$.

Consider ρ_1 and ρ_2 be the two T-SDHFNs. Let $S(\rho_1)$ and $S(\rho_2)$ be the score functions with $P(\rho_1)$ and $P(\rho_2)$ as the accuracy functions of ρ_1 and ρ_2 respectively. Then
If $S(\rho_1) > S(\rho_2)$ then $\rho_1 > \rho_2$
If $S(\rho_1) = S(\rho_2)$ then either $P(\rho_1) > P(\rho_2)$ then $\rho_1 > \rho_2$ or $P(\rho_1) = P(\rho_2)$ then $\rho_1 = \rho_2$

4. PROPOSED METHODOLOGY

In this study, LOPCOW method is applied to calculate the criterion weights and MUTRISS-II method is applied to rank the alternatives. The graphical representation of this framework is given in Fig. 1. Theoretical explanations of these methods are presented below.

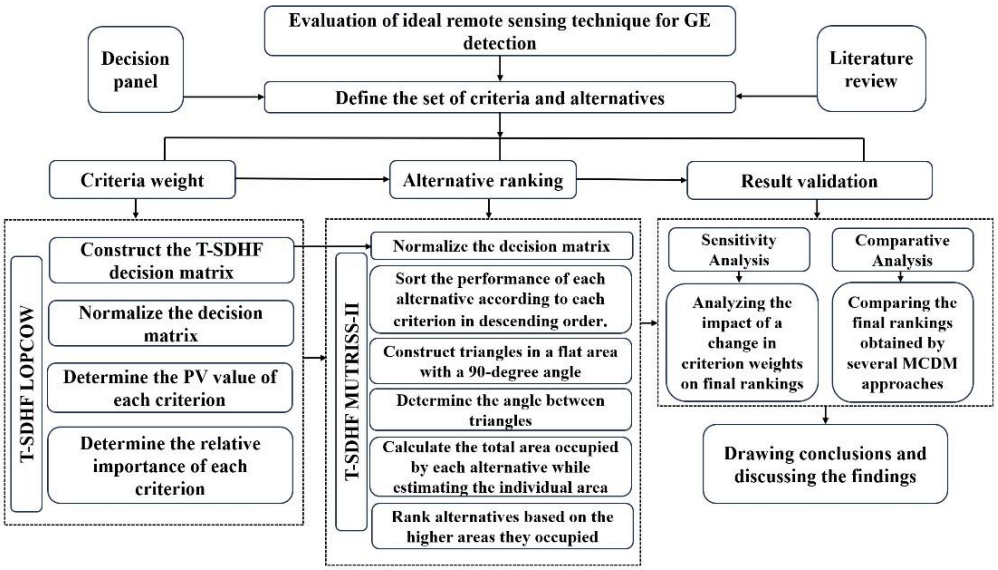

Fig. 1 Proposed MCDM framework

4.1. Logarithmic Percentage Change-Driven Objective Weighting Method

Step 1: Create the initial decision matrix,

$$D = \left[\wp_{ij} \right]_{m \times n} \tag{10}$$

here m and n represent the number of alternatives and criteria of the complex problem respectively. Each performance value $\wp_{ij}$ determined by the relevant experts are based on the T-SDHF set provided in Eq. (5). Then the T-SDHF decision matrix is defuzzified employing the score function provided in Eq. (8).

Step 2: The normalized decision matrix is determined by employing linear max-min normalization technique using the following equations,

$$R_{ij} = \begin{cases} \dfrac{\wp_{ij} - \wp_j^{\min}}{\wp_i^{\max} - \wp_i^{\min}} & \text{for beneficial criteria,} \\ \dfrac{\wp_j^{\max} - \wp_{ij}}{\wp_i^{\max} - \wp_i^{\min}} & \text{for cost criteria} \end{cases} \tag{11}$$

Step 3: The PV for every criterion is determined by taking the natural log of the mean square value and expressing it as a percentage of the standard deviation. This stage aids in reducing the weights' unequal distribution. As a result, PV is determined as,

$$\Im = \left| \ln \left(\frac{\sum_{i=1}^{m} \wp_{ij}^2}{\sigma} \right) \cdot 100 \right| \tag{12}$$

where the standard deviation and number of alternatives are denoted by σ and m respectively.

Step 4: The relative significance of each criterion is determined using the equation given below,

$$\aleph = \frac{\Im_{ij}}{\sum_{j=1}^{n} \Im_{ij}} \tag{13}$$

4.2. Multiple Triangles Scenarios-II Method

The algorithm for the i^{th} alternative in the proposed MUTRISS-II method is given as follows:

Step 1: The normalization of the matrix is done using the equation provided below,

$$\tilde{R}_{ij} = \begin{cases} \dfrac{\wp_{ij}}{\max\limits_{1\le j\le n} \wp_{ij}} & \text{for beneficial criteria} \\ \dfrac{\min\limits_{1\le j\le n} \wp_{ij}}{\wp_{ij}} & \text{for cost criteria} \end{cases} \tag{14}$$

Step 2: Construct the following equation by placing each $\wp_j$ of the i^{th} alternative in descending order,

$$\wp_{ij} : \wp_{mn_{\max}} \to \wp_{ij} \to \wp_{mn_{\min}} = \left\{ \wp_{mn_{\max}}, \wp_{mn_{\max-1}}, \cdots, \wp_{mn_{\min-n}}, \wp_{mn_{\min}} \right\} \tag{15}$$

Step 3: The subsequent equation is employed to compute the angles of each i^{th} alternative,

$$\theta_j = w_{\wp_{ij*}} \left(w_{\wp_{ij*}-1} \right)^{-1} \left(\sum w_{\wp_{ij*}} \left(w_{\wp_{ij*}-1} \right)^{-1} \right)^{-1} \times 90, \quad j = 1, \cdots, n-1 \tag{16}$$

$$w_{\wp_{ij*}} \succ w_{\wp_{ij*}-1}$$

Step 4: Calculate the overall score of the alternatives by calculating the areas that the alternatives occupy using the formula below,

$$AV_i = \sum_{j=1}^{n} w_{\wp_{ij*}} w_{\wp_{ij*}-1} \sin\theta_j 0.5 \tag{17}$$

in line with AV_i, the alternatives are arranged in descending order.

5. CASE STUDY

In this section, we have demonstrated the proposed novel hybrid MCDM approach through the selection of the most beneficial remote sensing technique for the exploration of geothermal reservoirs in India.

India, the third-largest global power consumer after the US and China, has an annual

demand of 1.54 trillion kWh, with over 45% met by fossil fuels, 26% by petroleum, and the rest from biomass and RE sources [49]. The country's large population drives increasing energy needs. Research by the Indian Institute of Science reveals 86 GW of installed RE capacity, including 34 GW from solar and 37.5 GW from wind power [49]. While solar and wind provide significant returns, their output can be inconsistent. A case study is conducted for the discovery of promising and untapped geothermal reservoirs in the Indian region.

To make sure that the DM process is strategic, and in line with the objective of identifying the most promising geothermal reservoir, an expert with insights in the pertinent field is selected to advise and validate the various remote sensing choices. Prior to extraction of the energy, a number of essential factors are taken into account to make an informed choice, the description of which is shown in Fig. 2.

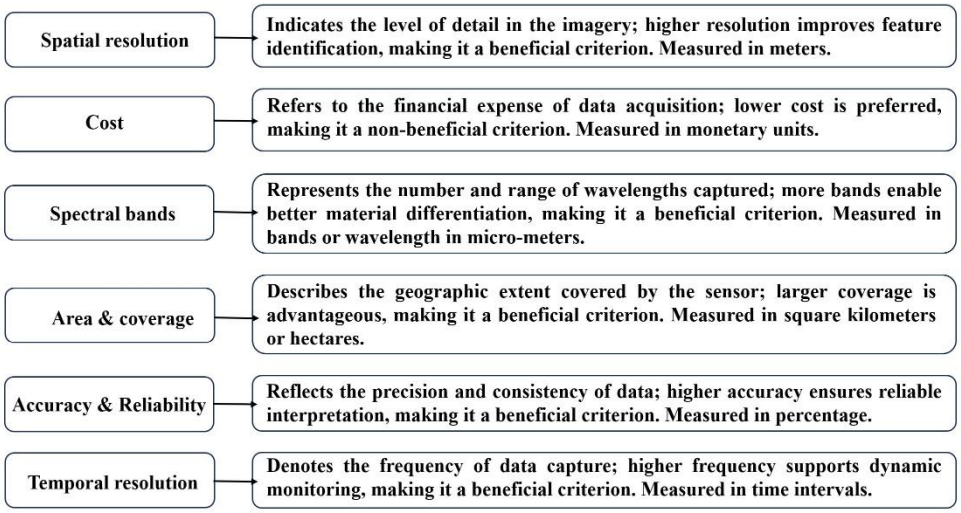

Fig. 2 Description of the criteria

The following gives a brief description about the remote sensing alternatives.

Light Detection and Ranging (LiDAR) (O_1) - The LiDAR remote sensing technique operates by producing laser pulses from an aerial or terrestrial platform and measuring the time it takes for the pulses to return after striking the Earth's surface. LiDAR sensors generate precise three-dimensional point clouds, allowing for thorough mapping of the Earth's topography and surface features. By providing realistic terrain models and recognizing structural patterns, LiDAR aids in mapping fractures, fault lines, and other subsurface features that may indicate the presence of geothermal reservoirs.

Thermal Infrared (TIR) (O_2) - This technique detects geothermal spots by gathering and analyzing thermal radiation released by the Earth's surface. The approach is based on sensors that capture infrared wavelengths linked with temperature fluctuations. The presence of underlying heat in geothermal locations causes various thermal signatures on the Earth's surface. TIR sensors detect these temperature variations, allowing for the exact identification of prospective geothermal areas. TIR sensing offers beneficial insights into the thermal properties of the landscape by measuring the heat emitted from the surface,

allowing for the recognition and mapping of regions with temperatures that are elevated, which indicate underlying geothermal activity.

RAdio Detection And Ranging (RADAR) (O_3) – This technique functions by radiating microwave pulses at the Earth's surface and capturing the signals that bounce back. RADAR is very valuable because it can penetrate clouds and function in all-weather situations. RADAR sensors can detect small surface deformations and topographical changes caused by subsurface geothermal activity. These modifications may include variations in ground elevation or surface roughness. The RADAR data can reveal these underlying structures, providing insights into feasible geothermal reservoirs.

Advanced Spaceborne Thermal Emission and Reflection Radiometer (ASTER) (O_4) – ASTER operates using multispectral and thermal infrared capabilities. In the context of geothermal detection, ASTER's thermal infrared bands (8-12 micrometers) are very relevant. These bands allow for the measurement of surface temperatures, which allows for the detection of thermal anomalies associated with probable geothermal locations. ASTER helps to identify and characterize subsurface heat sources by evaluating temperature changes and surface features. ASTER imagery's high degree of spatial accuracy makes it easier to identify geological structures and features essential to geothermal exploration.

Visible and Near-Infrared to Shortwave Infrared (VNIR, 350 to 1300 nm-SWIR, 1300 to 2500 nm) (O_5) – This remote sensing technology captures electromagnetic radiation in certain spectral bands extending from the visible to the shortwave infrared regions. Surface temperatures, vegetation and minerals all have distinct spectral signatures in these bands. VNIR bands are sensitive to differences in vegetation health and land cover, whereas SWIR bands are sensitive to temperature-related characteristics.

5.1. Determination of Criteria Weights

The developed fusion fuzzy MCDM framework is employed to determine the weights of each criterion and probable alternative. An expert in the pertinent field evaluates each of the alternatives O_i, i = 1, ..., 5, for the circumstance in hand in accordance with each of the attributes S_j, j = 1, ..., 6, and offers their assessment of performance in the form of a T-SDHFN. The steps adapted from the weighting and ranking technique is as follows:

Step 1: The expert evaluates each alternative's performance using the T-SDHFN specified in Eq. (5). Table 1 represents the initial T-SDHF matrix. Table 2 presents the defuzzified score matrix using the expression given in Eq. (5). An illustration of the score function of the first element (that is, $\wp_{11}$) is shown below,

$$\frac{\left(1+\left(\frac{1}{3}(0.52+0.26+0.15)-\frac{1}{2}(0.24+0.3)\right)^3-\left(\frac{1}{2}(0.35+0.5)-\frac{1}{2}(0.22+0.15)\right)^3\right)}{2}=0.4931$$

Step 2: The defuzzified matrix is normalized using the Eq. (11) for beneficial and cost criteria respectively.

$$R_{11}=\frac{0.4931-0.3862}{0.5096-0.3862}=0.8665$$

Table 1 The T-SDHF decision matrix

	S_1	S_2	S_3
O_1	(<{0.52,0.26,0.15},{0.24,0.30}>, <{0.52,0.36,0.66},{0.12,0.09}>, <{0.35,0.50},{0.22,0.15}>)	(<{0.39,0.29},{0.13}>, <{0.42},{0.14}>, <{0.26,0.31,0.45},{0.25,0.14,0.45}>)	(<{0.64,0.58,0.47},{0.15,0.21}>, <{0.15},{0.11}>, <{0.33,0.35},{0.14}>)
O_2	(<{0.45,0.67},{0.28}>, <{0.55,0.05},{0.31,0.43}>, <{0.25},{0.11}>)	(<{0.32},{0.19}>, <{0.15,0.25},{0.12,0.15}>, <{0.45,0.57,0.59},{0.17,0.35}>)	(<{0.34,0.67},{0.15,0.12,0.29}>, <{0.15,0.35},{0.19}>, <{0.25,0.35,0.45},{0.30,0.40,0.30}>)
O_3	(<{0.52,0.56},{0.33}>, <{0.62,0.53},{0.10,0.05}>, <{0.55},{0.36}>)	(<{0.43,0.37},{0.32}>, <{0.25,0.55},{0.13}>, <{0.47},{0.47,0.49}>)	(<{0.35},{0.11}>, <{0.47,0.15},{0.15}>, <{0.51,0.64},{0.15}>)
O_4	(<{0.39,0.41},{0.31}>, <{0.35,0.55},{0.21,0.34}>, <{0.25,0.34,0.48},{0.05,0.09}>)	(<{0.25},{0.12}>, <{0.15,0.35},{0.05,0.10}>, <{0.59,0.32},{0.36}>)	(<{0.15,0.39,0.25},{0.12,0.27}>, <{0.61,0.21},{0.05}>, <{0.42,0.34},{0.19}>)
O_5	(<{0.47,0.49},{0.26}>, <{0.69,0.15},{0.08}>, <{0.74},{0.20,0.05,0.11}>)	(<{0.35},{0.15}>, <{0.15,0.05},{0.60,0.40}>, <{0.40},{0.57}>)	(<{0.63,0.34},{0.11,0.09,0.13}>, <{0.21,0.15},{0.14}>, <{0.35,0.45},{0.06,0.21}>)

S_4	S_5	S_6
(<{0.68,0.55},{0.11}>, <{0.25,0.35},{0.17}>, <{0.37,0.15},{0.19,0.11}>)	(<{0.72,0.57},{0.16}>, <{0.15},{0.04}>, <{0.24,0.39},{0.14}>)	(<{0.69,0.75},{0.11,0.15}>, <{0.55},{0.14}>, <{0.51,0.15},{0.06,0.14}>)
(<{0.91,0.51},{0.04}>, <{0.34},{0.11}>, <{0.52,0.49},{0.24}>)	(<{0.65,0.54,0.61},{0.14,0.11}>, <{0.46},{0.22}>, <{0.62,0.49},{0.15,0.09}>)	(<{0.45,0.49,0.51},{0.21,0.14}>, <{0.45,0.35},{0.09,0.12}>, <{0.54},{0.30}>)
(<{0.59,0.43},{0.17}>, <{0.39,0.47},{0.11}>, <{0.43,0.41},{0.17,0.15,0.11}>)	(<{0.41,0.65},{0.26}>, <{0.45,0.55},{0.14,0.16}>, <{0.54},{0.08,0.31}>)	(<{0.61},{0.11}>, <{0.45,0.55},{0.04,0.16}>, <{0.65},{0.11,0.15}>)
(<{0.69,0.66,0.42},{0.11,0.21}>, <{0.55,0.65},{0.16,0.17}>, <{0.41,0.33,0.27},{0.14}>)	(<{0.61,0.59},{0.17}>, <{0.65},{0.20}>, <{0.61},{0.12}>)	(<{0.65,0.74},{0.18}>, <{0.65,0.55},{0.17,0.03}>, <{0.45,0.55,0.19},{0.13}>)
(<{0.79,0.57},{0.59}>, <{0.35,0.55},{0.33,0.01}>, <{0.15,0.25},{0.21}>)	(<{0.68,0.54},{0.31}>, <{0.35},{0.21}>, <{0.25,0.15},{0.10,0.16}>)	(<{0.65,0.75},{0.14,0.15}>, <{0.45},{0.11}>, <{0.15,0.45},{0.22,0.27}>)

Table 2 The defuzzified T-SDHF decision matrix

	S_1	S_2	S_3	S_4	S_5	S_6
O_1	0.4931	0.5045	0.5086	0.4995	0.5544	0.5966
O_2	0.5096	0.4905	0.5161	0.6411	0.5124	0.5077
O_3	0.5012	0.5003	0.4685	0.5091	0.4893	0.4922
O_4	0.4886	0.5007	0.4967	0.5360	0.4809	0.5588
O_5	0.3862	0.5065	0.5171	0.5744	0.5133	0.5854

Step 3: The PV of each criterion is computed using the Eq. (12) and is provided in Table 3. The PV of first criterion is given below,

$$\Im_1 = \left| \ln\left(\frac{0.8134}{0.3674}\right) \cdot 100 \right| = 79.4613$$

Step 4: Table 3 shows the relative significance of each criterion which is calculated using Eq. (13).

$$\aleph_1 = \frac{79.4613}{320.8675} = 0.2476$$

Table 3 Standard deviation, percentage value and significance of criteria

Criteria	σ	PV	Relative weight
S_1	0.3674	79.4613	0.2476
S_2	0.3452	38.9030	0.1212
S_3	0.3705	73.4468	0.2289
S_4	0.3643	35.5419	0.1108
S_5	0.3476	41.7180	0.1300
S_6	0.3975	51.7965	0.1614

5.2. Identifying the Rank of Alternatives

Step 1: A T-SDHF decision matrix is constructed in the form of Eq. (10) (refer Step 1 of LOPCOW method). The defuzzified matrix is normalized using the Eq. (14) for beneficial and cost criteria respectively. For instance,

$$\tilde{R}_{11} = \frac{0.4931}{0.5096} = 0.9677$$

Step 2: Each $\wp_j$ of i^{th} alternative is arranged in their descending order using Eq. (15). Table 4 shows the example of Alternative-1. That is, $\{S_6, S_5, S_3, S_2, S_1, S_4\}$.

Step 3: The angles of each triangle is computed using the Eq. (16). Table 4 shows the angles of each triangle for Alternative-1.

$$\theta_j = \left(0.1614 \times (1/13)\right) \times 0.1557 \times 90 = 17.3678$$

Step 4: Table 4 shows overall areas occupied by Alternative-1 using the Eq. (17). The angle and area occupied by rest of the alternatives are computed in the same way as Alternative-1. Table 5 shows the overall score and ranking of each alternative. For instance,

$$AV_1 = \left(1 \times 1 \times \sin(17.3978) \times 0.5\right) + 0.0681 + 0.2131 + 0.0562 + 0.1961 = 0.6831$$

Table 4 Area occupied by Alternative 1

Criteria	Alternative-1	Weight	Angle	θ_j	Radian	Area
S_6	1.0000	0.1614				
S_5	1.0000	0.1300	1.2416	17.3978	0.3038	0.1496
S_3	0.9837	0.2289	0.5680	7.9591	0.1390	0.0681
S_2	0.9722	0.1212	1.8879	26.4549	0.4619	0.2131
S_1	0.9677	0.2476	0.4896	6.8603	0.1198	0.0562
S_4	0.7792	0.1108	2.2357	31.3279	0.5470	0.1961
						0.6831

Table 5 Rank and area occupied by each alternative

Alternative	AV_i	Rank
O_1	0.6831	3
O_2	0.7187	1
O_3	0.6252	5
O_4	0.6532	4
O_5	0.6914	2

6. Results and Discussion

In this study, the optimal RS technique for the maximal energy detection of the geothermal reservoir is explored through novel hybrid fuzzy MCDM under a T-SDHF environment.

The spherical framework of the T-SDHF set enabled a smoother transition between varying levels of uncertainty. By incorporating the flexibility of DHF set, which accommodated multiple membership and non-membership degrees, the T-SDHF set accurately depicted complex and multidimensional data, by allowing choice-makers to capture intricate interconnections within a decision context. In scenarios where standard fuzzy sets or HF sets, which address only membership hesitation, fall short, the T-SDHF set provides a more comprehensive solution. T-SDHF set-based techniques additionally enhanced DM resilience by providing a systematic framework for dealing with ambiguities and vagueness, hence increasing the dependability and stability of decision outputs.

The case study in this research involved six criteria and five alternatives. The significance of each criterion was computed using the T-SDHF LOPCOW method, and the ranking of the alternatives was done using the MUTRISS-II method. The LOPCOW approach leverages objective information to generate the criteria weights. The criterion weights have a relatively even distribution. Furthermore, this technique proves to efficiently handle an enormous number of parameters and alternatives. Contrarily, MUTRISS-II gets beyond the shortcomings of the existing MCDM approach, which include inconsistent ranking, identifying several possibilities as preferred alternatives, and failing to consider the input of experts during the DM process. The versatility of the suggested hybrid technique, as well as its ability to give precise information, contribute to its usefulness in assisting geothermal exploration DM. Furthermore, the proposed approach aims to provide accurate solutions using robust but simple algorithmic procedures.

From the results of the T-SDHF LOPCOW method, it is found that spatial resolution (S_1) obtained the highest weightage of 0.2476, followed by spectral bands (S_3) with a value of 0.2289, and thirdly temporal resolution (S_6) with 0.1614. The spatial resolution determined the level of clarity in the image. It accurately detected tiny features such as temperature anomalies and surface manifestations, which were critical for identifying probable geothermal sites. On the other hand, even though the area with coverage (S_4) of the distinct remote sensing techniques were significant, this criterion obtained the least value of 0.1108.

TIR (O_2) obtained 0.7187 and constituted the leading remote sensing technique for identifying geothermal reserves. TIR has the ability to detect small temperature variations, which is critical for efficient and targeted geothermal exploration and resource assessment. TIR sensing provides unique insights into the thermal features of the landscape by

measuring heat released from the surface, allowing for the identification and mapping of areas with elevated temperatures that indicate underlying geothermal activity. The TIR remote sensing for detecting potential geothermal sites is shown in Fig. 3. Different triangles covered by TIR are displayed in Fig. 4.

The second favored technique was VNIR-SWIR (O_5), which achieved a value of 0.6914. These sensors are very useful for studying the Earth's surface features. The technique uses sensitivity to detect minor changes in surface composition and temperature that indicate geothermal activity. VNIR-SWIR remote sensing identifies and maps probable geothermal energy locations by analyzing reflectance patterns and thermal anomalies.

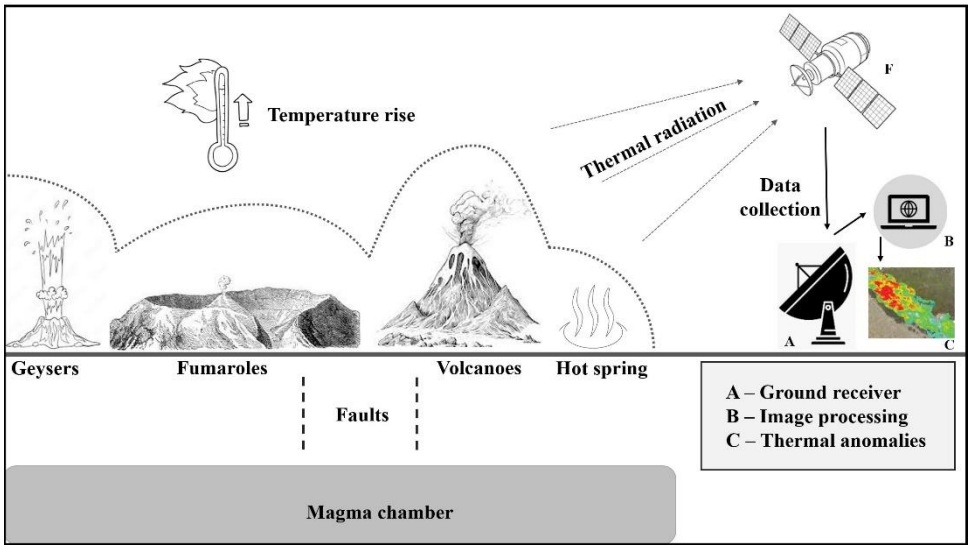

Fig. 3 TIR detecting heat anomalies

Even though LiDAR (O_1) is extremely accurate for topographic mapping, it is limited by its reliance on direct line-of-sight. This means that elements obscured by dense foliage or structures may not be fully recorded. Furthermore, LiDAR data collecting and processing can be expensive and resource-intensive, providing obstacles for projects with little funding. This puts LiDAR in third place for geothermal location detection. ASTER has a limited revisit frequency, which means that revisit times might be relatively long, ranging from weeks to months depending on the location. This infrequent visitation complicates the monitoring of dynamic geothermal phenomena that may change rapidly over shorter timescales. Whereas RADAR's (O_3) poor ability to penetrate dense foliage limits its effectiveness in heavily forested areas. Furthermore, RADAR often has lower spatial resolution than optical sensors such as ASTER (O_4). This places ASTER fourth, with RADAR being the least recommended alternative.

Despite TIR's high ranking in geothermal resource exploration, challenges persist due to the ill-posed nature of surface temperature data, which is constrained by limited spectral information and assumptions about air conditions or emissivity. To address these limitations, it is crucial to integrate multiple remote sensing methods such as optical,

infrared, and radar and employ high-spectral TIR imaging for comprehensive data fusion [50].

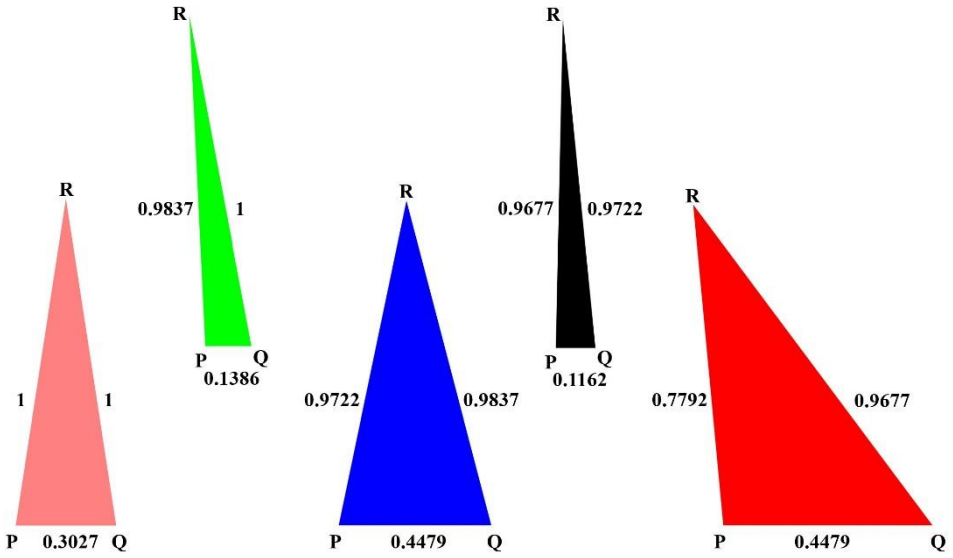

Fig. 4 Different triangles covered by TIR

This approach enhances the accuracy and consistency of geothermal resource exploration by mitigating issues like uneven surface temperatures and atmospheric interference. Combining data from various sensors and increasing observation frequencies can provide more precise insights and capture complex geothermal resource characteristics.

This study benefits stakeholders and the government by highlighting the risks of inaccurate geothermal reserve estimation. Overestimating reserves may lead to excessive costs and environmental impact, while underestimating them could cause premature operation shutdowns and financial losses. Erroneous forecasts can also hinder reservoir management, threatening long-term sustainability.

6.1. Comparative Analysis of Different Ranking Techniques

Every MCDM technique has a unique way for carrying out DM examination. In this section, the outcomes of the proposed hybrid MCDM methodology are compared to those of existing MCDM techniques. We compared the rankings of our proposed technique to distance-based (TOPSIS) [15], score-additive (COPRAS) [51], trace-based (MCRAT) [52], perimeter similarity (RAPS) [53], outranking (PROMETHEE-II) [16], and aggregated sum product (WASPAS) [18] methods.

From Table 6, it is seen that O_2 consistently ranks as the highest performing alternative in most methods. For instance, in the TOPSIS method, O_2 has the highest score, compared to O_1, O_3, O_4, and O_5, indicating that it is the most optimal choice based on relative closeness to the ideal solution. Similarly, in COPRAS, O_2 achieves a perfect score of 1, outperforming the other alternatives. In contrast, the MCRAT method shows a smaller gap between alternatives, with O_1 (0.1780) and O_2 (0.1787) having nearly identical values, but

O_2 still slightly edges ahead. For the RAPS method, O_2 remains the best performer, while O_1 is worst. In the PROMETHEE-II method, O_2 also outperforms all other alternatives with a positive value of 0.038, while O_3, O_4, and O_5 have negative values, indicating poorer relative performance. Lastly, in the WASPAS method, O_2 marginally outperforms O_1, but the difference between the alternatives is minimal overall.

Table 6 Comparison of the proposed model with the existing models

	TOPSIS	COPRAS	MCRAT	RAPS	PROMETHEE-II	WASPAS
O_1	0.6956	0.9932	0.1780	0.9692	0.0314	0.4802
O_2	0.7239	1.0000	0.1787	0.9753	0.0380	0.4829
O_3	0.5480	0.9366	0.1688	0.9244	-0.0370	0.4529
O_4	0.6355	0.9647	0.1730	0.9454	-0.0033	0.4664
O_5	0.3710	0.9438	0.1664	0.9117	-0.0291	0.4560

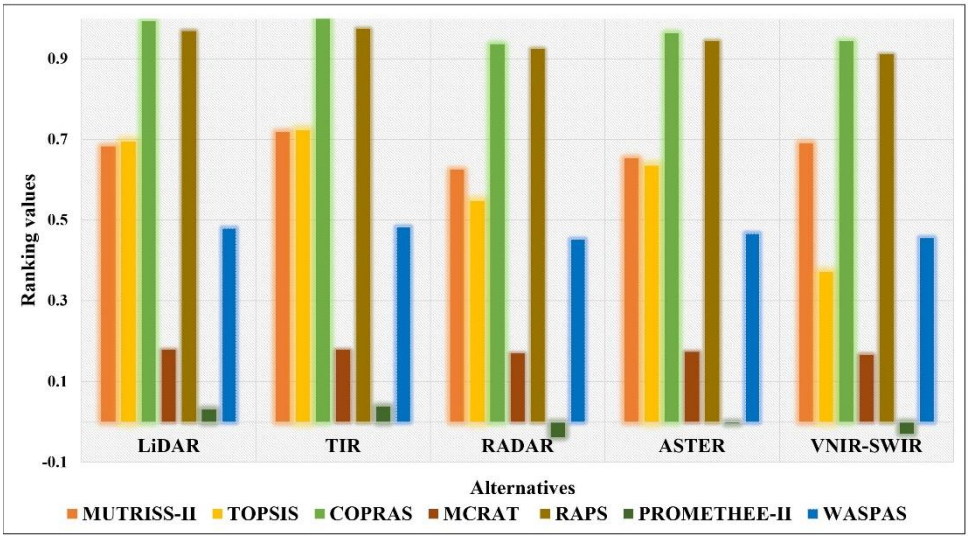

Fig. 5 Comparison of the proposed technique with existing models

The variation in rankings across these methods highlights the sensitivity of the results to the chosen decision-making approach, emphasizing the need to select the method that best aligns with the decision context and priorities. The results reveal that the integrated MCDM framework produces more flexible solutions than the individual techniques. However, in contrast to the aforementioned MCDM methodologies, the suggested strategy is compatible for our application. Fig. 5 shows a grouped bar plot illustrating the ranks acquired using various MCDM approaches. To go deeper into these rankings, Spearman's rank correlation coefficient is employed. Fig. 6 shows the results of the correlation coefficient.

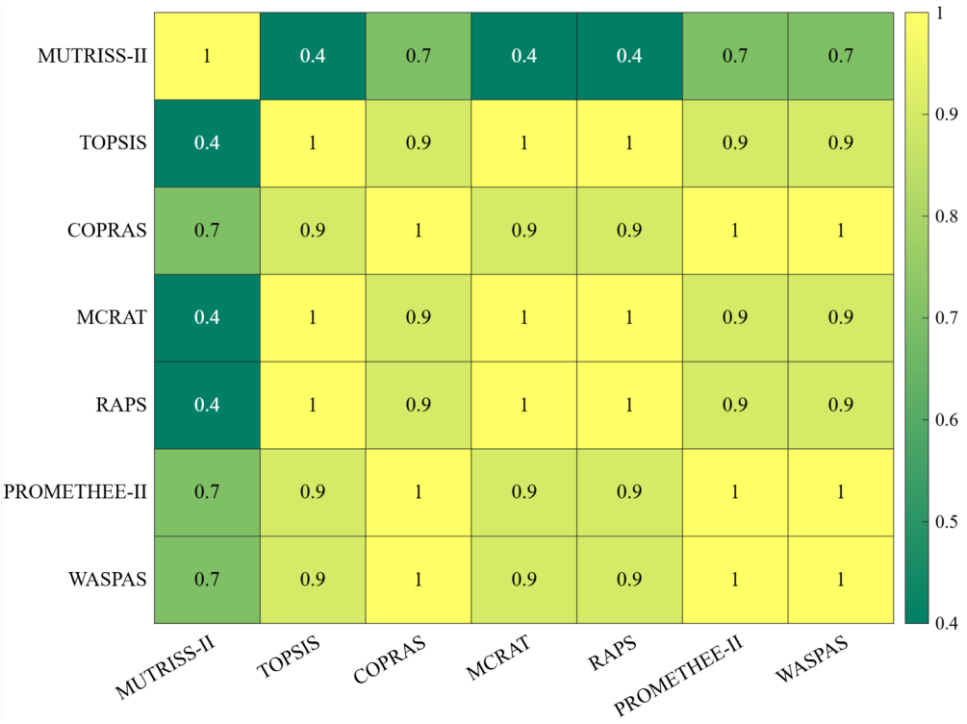

Fig. 6 Spearman's rank correlation coefficient

6.2. Sensitivity Analysis

In this section, we evaluated the level of sensitivity of our suggested system. The coherence of the findings obtained with the proposed approach is assessed by varying the significance level of each criterion. To evaluate the reliability of the gathered results, we examine two cases.

In the first case, the beneficial criteria, high desired value, is set to one, while the cost criteria, least desired value, is assigned to zero. That is, S_1, S_3, S_4, S_5, S_6, which are considered as the beneficial criteria are given the value of 0.2 and the cost criterion, namely, (S_2) is asset to zero. In the second case, both the beneficial and non-beneficial criteria are set to be equal. Here, all the criteria are assigned equal values of 0.167.

Table 7 and Fig. 7 illustrate the impact of adjusting significant parameters on the ranking of alternatives in two different cases, highlighting the responsiveness of the model to changes in criterion weighting. In Case-I, the alternatives are ranked as follows: O_4 is the top choice followed by O_5, O_3, O_1, and O_2 in the last position. In Case-II, however, the rankings change considerably: O_4 remains the highest ranked, but O_2 rises to the second position, followed closely by O_3, O_5, and O_1 drops to the lowest rank. These shifts demonstrate that even slight variations in the weighting of criteria can lead to a reordering of alternatives, emphasizing the model's sensitivity to the values assigned to different factors. This investigation underlines the importance of proper weight adjustment to ensure that the chosen alternative aligns with the desired priorities in each scenario.

Table 7 Results of the sensitive analysis

Alternative	Case - I		Case - II	
	AV_i	Rank	AV_i	Rank
O_1	0.0170	4	0.02146	5
O_2	0.0164	5	0.02151	2
O_3	0.0181	3	0.02149	3
O_4	0.0233	1	0.02152	1
O_5	0.0200	2	0.02148	4

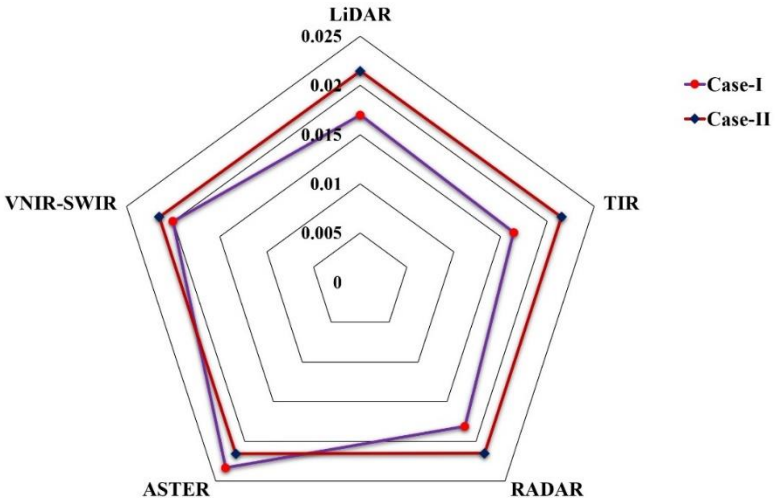

Fig. 7 Radar representation of the outcome of sensitive analysis

Further, Spearman rank correlation coefficient was conducted in the study. It showed that the proposed rank showed a negative correlation of -0.5 with Case-I, indicating a moderate inverse relationship between the two. Similarly, the proposed rank and Case-II exhibited a negative correlation of -0.1, suggesting a very weak inverse association. In contrast, the correlation between Case-I and Case-II was positive, with a value of 0.3, indicating a weak positive relationship between the two cases. These results provide insights into how the different cases and the proposed rank interact and highlight varying degrees of association among them.

7. CONCLUSION

As the entire world grapples with the challenges of a burgeoning population, the transition to RE emerges as a critical strategy for ensuring a robust and sustainable future. The need to investigate different sources of RE is critical for producing energy in situations where the conventional high energy return renewable resources become inconsistent and unreliable. In this study, geothermal reserves were identified using the most promising RS approach through a unique hybrid fuzzy MCDM technique. One of the distinguishing features of the GE is its reliability and consistency. Geothermal power generation, unlike

other RE sources such as solar or wind, is not weather-dependent. It delivers continuous and baseload power, making it an important and consistent contributor to the global energy mix. RS technologies allow for the detailed mapping of surface temperatures, geological formations, and vegetation stress, which are indicators of geothermal activity. This minimizes the need for extensive ground-based surveys and drilling, reducing environmental disruption and lowering exploration costs. Additionally, continuous monitoring through RS supports the efficient management of geothermal fields, ensuring the long-term viability and minimal ecological impact of geothermal energy projects. The T-SDHF-LOPCOW-MUTRISS-II model is used to assess the difficulty of selecting an appropriate remote sensing technique for detecting probable geothermal reserves in India.

Understanding the characteristics of geothermal spots prior to extraction is critical for drilling activities to reduce the risk of resource depletion or reservoir damage, thereby contributing to the overall sustainability, efficiency, and responsible management of GE resources. Therefore, five RS techniques were investigated under several critical criteria in a newly introduced T-SDHF environment. The combination of the T-SF set with the DHF set has proven to be a promising technique for dealing with ambiguity as well as vagueness in the DM process. The LOPCOW approach assessed the relative importance of each crucial criterion. The LOPCOW results revealed that spatial resolution and area with coverage were the most and least critical parameters for precisely locating the site for maximum energy extraction. MUTRISS-II method uses triangles to express criteria-based performance values and prioritizes remote sensing approaches based on the area of the shapes formed by these triangles. The angles between the triangles are dynamically calculated in MUTRISS-II. This technique revealed that the TIR approach improved the ability to identify minor temperature differences in a concise manner, allowing for more efficient exploration and usage of geothermal resources. This approach also offered useful information on the thermal properties of the ground. According to the sensitivity analysis, the suggested method is sensitive to the weights of the attributes, and the comparative analysis confirmed that our established structure is capable of providing a reliable remote sensing technique for potential geothermal reserves.

This study, like many other scientific investigations, has some limitations. The data focused solely on prospective RS techniques for exploring geothermal resources in the Indian region, and only one DM expert was involved, limiting the breadth of informed DM. Additionally, the novel MUTRISS-II approach, which utilized analytic geometry to determine areas filled by alternatives in n-dimensional space, struggled with handling unknown variables in the application. While TIR is the top strategy for exploring geothermal resources, it might be challenging to obtain data just from this method. Surface temperature estimation is challenging due to limited spectral information and assumptions about air conditions or emissivity, resulting in inaccurate results. To overcome this constraint, varied RS data must be integrated.

Future research could broaden the scope by incorporating data from countries across various regions of the world and enhancing the analysis process by including group knowledge. Interdisciplinary research is crucial for exploring and evaluating geothermal resources. Collaboration among geology, geophysics, geochemistry, geography, and hydrology enhances resource detection accuracy and provides a comprehensive assessment of potential, providing reliable foundations for energy development. Furthermore, the newly developed set could also be extended to incorporate other subjective weighting methods or MCDM techniques for identifying potential geothermal sites.

Acknowledgement: *This work was supported by the Ministry of Education of the Republic of Korea and National Research Foundation of Korea (NRF) (NRF-2024S1A5A8028933).*

REFERENCES

1. da Cunha Dias, T.A., Lora, E.E.S., Maya, D.M.Y., del Olmo, O.A., 2021, *Global potential assessment of available land for bioenergy projects in 2050 within food security limits*, Land Use Policy, 105, 105346.
2. Petrov, S., Aleksandrova, S., Kirova, S., 2024, *Environmental effects of green bonds and other forms of financing in the European union*, International Journal of Economic Sciences, 13(1), pp. 81-105.
3. Chhandama, M.V.L., Satyan, K.B., Changmai, B., Vanlalveni, C., et al., 2021, *Microalgae as a feedstock for the production of biodiesel: A review*, Bioresource Technology Reports, 15, 100771.
4. Rohit, R.V., Kiplangat, D.C., Veena, R., Jose, R., et al., 2023, *Tracing the evolution and charting the future of geothermal energy research and development*, Renewable and Sustainable Energy Reviews, 184, 113531.
5. Zhu, J., Hu, K., Lu, X., Huang, X., et al., 2015, *A review of geothermal energy resources, development, and applications in China: Current status and prospects*, Energy, 93, pp. 466-483.
6. Ahmed, I., Liu, H., Chen, R., Ahmad, J., et al., 2024, *Geothermal resource exploration in Reshi town by integrated geophysical methods*, Energies, 17(4), 856.
7. Ghoneim, E., Healey, C., Hemida, M., Shebl, A., et al., 2023, *Integration of geophysical and geospatial techniques to evaluate geothermal energy at Siwa oasis, western desert, Egypt*, Remote Sensing, 15(21), 5094.
8. Yang, Y., Xiong, B., Peng, S., Chen, H., et al., 2023, *Geothermal exploration using numerical simulation and a comprehensive electromagnetic method*, Petroleum Science and Technology, 41(3), pp. 361-385.
9. Qin, Q., Zhang, N., Nan, P., Chai, L., 2011, *Geothermal area detection using Landsat ETM+ thermal infrared data and its mechanistic analysis-A case study in Tengchong, China*, International Journal of Applied Earth Observation and Geoinformation, 13(4), pp. 552-559.
10. Mishra, A.R., Rani, P., Cavallaro, F., Alrasheedi, A.F., 2023, *Assessment of sustainable wastewater treatment technologies using interval-valued intuitionistic fuzzy distance measure-based MAIRCA method*, Facta Universitatis, Series: Mechanical Engineering, 21(3), pp. 359-386.
11. Ali, Z., 2025, *Fairly Aggregation operators based on complex p, q-rung orthopair fuzzy sets and their application in decision-making problems*, Spectrum of Operational Research, 2(1), pp. 113-131.
12. Sarfraz, M., 2024, *Application of interval-valued t-spherical fuzzy Dombi Hamy mean operators in the antiviral mask selection against COVID-19*, Journal of Decision Analytics and Intelligent Computing, 4(1), pp. 67-98.
13. Lo, H.W., Chan, H.W., Lin, J.W., Lin, S.W., 2024, *Evaluating the interrelationships of industrial 5.0 development factors using an integration approach of Fermatean fuzzy logic*, Journal of Operations Intelligence, 2(1), pp. 95-113.
14. Gul, R., 2025, *An extension of VIKOR approach for MCDM using bipolar fuzzy preference δ-covering based bipolar fuzzy rough set model*, Spectrum of Operational Research, 2(1), pp. 72-91.
15. Dinçer, H., Yüksel, S., Eti, S., 2023, *Identifying the right policies for increasing the efficiency of the renewable energy transition with a novel fuzzy decision-making model*, Journal of Soft Computing and Decision Analytics, 1(1), pp. 50-62.
16. Sotiropoulou, K.F., Vavatsikos, A.P., Botsaris, P.N., 2024, *A hybrid AHP-PROMETHEE II onshore wind farms multicriteria suitability analysis using kNN and SVM regression models in northeastern Greece*, Renewable Energy, 221, 119795.
17. Kang, D., Suvitha, K., Narayanamoorthy, S., Sandra, M., et al., 2024, *Evaluation of wave energy converters based on integrated ELECTRE approach*, Expert Systems with Applications, 242, 122793.
18. Madić, M., Petrović, G., Petković, D., Janković, P., 2024, *Traditional and integrated MCDM approaches for assessment and ranking of laser cutting conditions*, Spectrum of Mechanical Engineering and Operational Research, 1(1), pp. 250-257.
19. Więckowski, J., Sałabun, W., 2025, *Comparative sensitivity analysis in composite material selection: Evaluating OAT and COMSAM methods in multi-criteria decision-making*, Spectrum of Mechanical Engineering and Operational Research, 2(1), pp. 1-12.
20. Komatina, N., Marinkovic, D., Tadic, D., Pamucar, D., 2025, *Advancing PFMEA Decision-Making: FRADAR Based Prioritization of Failure Modes Using AP, RPN, and Multi-Attribute Assessment in the Automotive Industry*, Tehnicki Glasnik, accepted for publication.

21. Bouraima, M.B., Ibrahim, B., Qiu, Y., Muhammad, L.J., et al., 2024, *Assessment of solar energy technologies in meeting the 2030 agenda and sustainable development goals under an interval-valued Fermatean fuzzy environment*, Journal of Operations Intelligence, 2(1), pp. 114-128.
22. Qian, S., Qiu, Y., Bouraima, M.B., Badi, I., et al., 2024, *Assessing the challenges to leverage carbon markets for renewable energy in developing countries: A multi-criteria decision-making approach*, Spectrum of Engineering and Management Sciences, 2(1), pp. 151-160.
23. Yüksel, S., Eti, S., Dinçer, H., Gökalp, Y., 2024, *Comprehensive risk analysis and decision-making model for hydroelectricity energy investments*, Journal of Soft Computing and Decision Analytics, 2(1), pp. 28-38.
24. Kousar, S., Ansar, A., Kausar, N., Freen, G., 2024, *Multi-criteria decision-making for smog mitigation: A comprehensive analysis of health, economic, and ecological impacts*, Spectrum of Decision Making and Applications, 2(1), pp. 53-67.
25. Ecer, F., Pamucar, D., 2022, *A novel LOPCOW-DOBI multi-criteria sustainability performance assessment methodology: An application in developing country banking sector*, Omega, 112, 102690.
26. Tadic, D., Lukic, J., Komatina, N., Marinkovic, D., Pamucar, D., 2025, 2023, *A Fuzzy Decision-Making Approach to Electric Vehicle Evaluation and Ranking*, Tehnicki Vjesnik, 32(3), pp. 1066-1075.
27. Nila, B., Roy, J., 2023, *A new hybrid MCDM framework for third-party logistic provider selection under sustainability perspectives*, Expert Systems with Applications, 234, 121009.
28. Ulutaş, A., Topal, A., Görçün, Ö.F., Ecer, F., 2024, *Evaluation of third-party logistics service providers for car manufacturing firms using a novel integrated grey LOPCOW-PSI-MACONT model*, Expert Systems with Applications, 241, 122680.
29. Biswas, S., Joshi, N., 2023, *A performance-based ranking of Initial Public Offerings (IPOs) in India*, Journal of Decision Analytics and Intelligent Computing, 3(1), pp. 15–32.
30. Sahoo, S.K., Goswami, S.S., 2023, *A comprehensive review of multiple criteria decision-making (MCDM) methods: Advancements, applications, and future directions*, Decision Making Advances, 1(1), pp. 25-48.
31. Zakeri, S., Chatterjee, P., Cheikhrouhou, N., Konstantas, D., et al., 2023, *MUTRISS: A new method for material selection problems using MUltiple-TRIangles scenarios*, Expert Systems with Applications, 228, 120463.
32. Pelissari, R., Khan, S.A., Ben-Amor, S., 2022, *Application of multi-criteria decision-making methods in sustainable manufacturing management: A systematic literature review and analysis of the prospects*, International Journal of Information Technology & Decision Making, 21(02), pp. 493-515.
33. Lin, M., Li, X., Chen, R., Fujita, H., et al., 2022, *Picture fuzzy interactional partitioned Heronian mean aggregation operators: An application to MADM process*, Artificial Intelligence Review, 55, pp. 1-38.
34. Kutlu Gündoğdu, F., Kahraman, C., 2019, *Spherical fuzzy sets and spherical fuzzy TOPSIS method*, Journal of Intelligent & Fuzzy Systems, 36(1), pp. 337-352.
35. Bonab, S.R., Ghoushchi, S.J., Deveci, M., Haseli, G., 2023, *Logistic autonomous vehicles assessment using decision support model under spherical fuzzy set integrated Choquet integral approach*, Expert Systems with Applications, 214, 119205.
36. Nguyen, P.H., Nguyen, L.A.T., Pham, H.A.T., Pham, M.A.T., 2023, *Breaking ground in ESG assessment: Integrated DEA and MCDM framework with spherical fuzzy sets for Vietnam's wire and cable sector*, Journal of Open Innovation: Technology, Market, and Complexity, 9(3), 100136.
37. Gamal, A., Abdel-Basset, M., Hezam, I.M., Sallam, K.M., et al., 2024, *A computational sustainable approach for energy storage systems performance evaluation based on spherical-fuzzy MCDM with considering uncertainty*, Energy Reports, 11, pp. 1319-1341.
38. Riaz, M., Hashmi, M.R., Pamucar, D., Chu, Y.M., 2021, *Spherical linear diophantine fuzzy sets with modeling uncertainties in MCDM*, Computer Modeling in Engineering & Sciences, 126(3), pp. 1125-1164.
39. Kakati, P., Quek, S.G., Selvachandran, G., Senapati, T., et al., 2024, *Analysis and application of rectified complex t-spherical fuzzy Dombi-Choquet integral operators for diabetic retinopathy detection through fundus images*, Expert Systems with Applications, 243, 122724.
40. Alamoodi, A.H., Albahri, O.S., Deveci, M., Albahri, A.S., et al., 2024, *Selection of electric bus models using 2-tuple linguistic t-spherical fuzzy-based decision-making model*, Expert Systems with Applications, 249, 123498.
41. Supriya, Y., Gadekallu, T.R., 2023, *A survey on soft computing techniques for federated learning-applications, challenges and future directions*, ACM Journal of Data and Information Quality, 15(2), pp. 1-28.
42. Mostafaeipour, A., Hosseini Dehshiri, S.J., Hosseini Dehshiri, S.S., Jahangiri, M., et al., 2020, *A thorough analysis of potential geothermal project locations in Afghanistan*, Sustainability, 12(20), 8397.
43. Puppala, H., Jha, S.K., Singh, A.P., Elavarasan, R.M., et al., 2022, *Identification and analysis of barriers for harnessing geothermal energy in India*, Renewable Energy, 186, pp. 327-340.

44. Ghose, D., Pradhan, S., Shabbiruddin., 2022, *Development of model for assessment of renewable energy sources: A case study on Gujarat, India*, International Journal of Ambient Energy, 43(1), pp. 1157-1166.
45. Gudala, M., Govindarajan, S.K., Tariq, Z., Yan, B., 2023, *Numerical investigations and evaluation of a Puga geothermal reservoir with horizontal wells using a fully coupled thermo-hydro-geo-mechanical model (THM) and EDAS associated with AHP*, Geo-energy Science and Engineering, 228, 212035.
46. Nematollahi, B., Chen, M., Nikoo, M.R., Al-Maktoumi, A., 2023, *Evaluation and optimization of a horizontal well-triplet for CO_2 plume geothermal harvest: Comparison between open and close reservoirs*, Journal of Hydrology, 623, 129811.
47. Ng'ethe, J., Jalilinasrabady, S., 2023, *GIS-based multi-criteria decision making under silica saturation index (SSI) for selecting the best direct use scenarios for geothermal resources in central and southern Rift valley, Kenya*, Geothermics, 109, 102656.
48. Zorlu, K., Dede, V., 2023, *Assessment of glacial geoheritage by multi-criteria decision making (MCDM) methods in the Yalnızçam mountains, Northeastern Türkiye*, International Journal of Geoheritage and Parks, 11(1), pp. 100-117.
49. Pradhan, S., Ghose, D., 2023, *An integrated approach to rank prospective sites for wind-powered pumped storage hydroelectric plants to meet rising demand in the Indian subcontinent*, Journal of Energy Storage, 72, 108474.
50. Wang, S., Xu, W., Guo, T., 2024, *Advances in thermal infrared remote sensing technology for geothermal resource detection*, Remote Sensing, 16(10), 1690.
51. Sagiroglu, A., Demir, M.C., Taskin, A., 2024, *Assessing collaboration performance of NGOs by a decomposed fuzzy approach utilizing AHP and COPRAS methods: Turkiye case*, International Journal of Disaster Risk Reduction, 111, 104744.
52. Stević, Ž., Ersoy, N., Başar, E.E., Baydaş, M., 2024, *Addressing the global logistics performance index rankings with methodological insights and an innovative decision support framework*, Applied Sciences, 14(22), 10334.
53. Saleh, N., Hassan, M.A., Salaheldin, A.M., 2024, *Skin cancer classification based on an optimized convolutional neural network and multicriteria decision-making*, Scientific Reports, 14(1), 17323.